ELSEVIER

International Journal of Pharmaceutics 129 (1996) 159–173

international journal of pharmaceutics

Crystallization tendency and polymorphic transitions in triglyceride nanoparticles

Heike Bunjes[a,*], Kirsten Westesen[a], Michel H.J. Koch[b]

[a]*Institute for Pharmacy, Department for Pharmaceutical Technology, Friedrich-Schiller University Jena, Lessingstrasse 8, D-07743 Jena, Germany*

[b]*European Molecular Biology Laboratory, Hamburg Outstation, EMBL c/o DESY, Notkestrasse 85, D-22603 Hamburg, Germany*

Received 14 June 1995; accepted 16 August 1995

Abstract

The ability of tristearin, tripalmitin, trimyristin and trilaurin to form solid lipid nanoparticles after melt-homogenization is investigated by DSC and X-ray diffraction. Upon storage at common temperatures after preparation solid nanoparticles are formed in tristearin and tripalmitin dispersions. In contrast to literature reports, colloidal dispersions of trilaurin do not form solid particles under those conditions. They should, therefore, be regarded as emulsions of supercooled melts rather than as nanosuspensions. Trimyristin nanoparticles which can be obtained in solid or liquid form have a larger incorporation capacity for the lipophilic model drug menadione in the liquid than in the solid state. The kinetics of polymorphic transitions after crystallization of triglyceride nanoparticles are slower for longer-chain than for shorter-chain triglycerides. Addition of tristearin raises the crystallization temperature of colloidally dispersed trimyristin and trilaurin facilitating solidification during production. The structure and melting behavior of the resulting mixed nanoparticles are more complex than those of nanoparticles prepared from the simple triglycerides. Depending on the mixing ratio, the time-course of polymorphic transitions after crystallization may also be altered significantly. The melting enthalpy of the mixed nanoparticle dispersions is usually not significantly different from that of dispersions of the simple triglycerides.

Keywords: Colloidal drug carrier; Nanoparticle; Supercooled melt; Emulsion; Triglyceride

1. Introduction

Nanoparticles prepared from lipids solid at room temperature have been proposed as a new type of drug carrier system (Siekmann and Westesen, 1992). They can be obtained by homogenizing a molten lipid in an aqueous phase containing physiologically compatible emulsifiers such as phospholipids, bile salts and poloxamers as stabilizers. Several materials such as saturated monoacid triglycerides or hard fats have been used as matrix for lipid nanoparticles (Siekmann and Westesen, 1992; Müller et al., 1995). Solid lipid particle systems are supposed to be biodegradable, non-toxic, stable against coalescence and drug leakage and to have a matrix-con-

* Corresponding author. Tel.: +49 3641 636781; Fax: +3641 636766.

SSDI 0378-5173(95)04286-J

trolled drug delivery. Particle sizes in the nanometer range may allow parenteral and even intravenous administration.

The properties of colloidally dispersed glycerides differ from those of their bulk materials due to their colloidal size. This especially applies to the melting and crystallization behavior and to the kinetics of polymorphic transitions (Westesen et al., 1993; Siekmann and Westesen, 1994a; Westesen and Bunjes, 1995). Concerning the production process, the pronounced supercooling tendency of the nanoparticles is of major importance since potential advantages of these systems such as sustained drug release essentially rely on the solid state of the lipid matrix. Solidification of the particles after melt-homogenization must, therefore, be ensured. It has to be taken into consideration, however, that some lipid materials may not crystallize in the colloidally dispersed state. In this case, the dispersions should in fact be regarded as emulsions of supercooled melts rather than as dispersions of solid particles. It is the aim of the present study to investigate the ability of triglycerides to form nanoparticles with the desired properties. The resulting particles should crystallize under controlled conditions during production to yield a solid matrix. It would be favorable if the particles remain in the solid state at body temperature to allow sustained drug release. Knowledge about the processing behavior of a range of different triglycerides may help to understand the processes in other triglycerides and more complex mixtures. It should also be evaluated if a correlation between the behavior in bulk and dispersed state can be derived. For simplicity, the series of saturated even monoacid triglycerides with a chain length between 12 and 18 carbons was chosen for the present study. These triglycerides seem promising for the preparation of solid lipid nanoparticles because their melting points are above body temperature but sufficiently low to allow melt-homogenization in an aqueous phase. To evaluate the impact of the physical state on the drug incorporation capacity of triglyceride nanoparticles the incorporation capacity of solid particles is compared to that of emulsified triglycerides using menadione as a lipophilic model drug.

Crystallization of bulk triglycerides from the melt after rapid cooling usually occurs in the metastable α-form which transforms via the β'- into the stable β-form upon heating or storage. In colloidally dispersed triglycerides these transitions are faster than in the bulk and their course may be altered (Westesen et al., 1993; Siekmann and Westesen, 1994a; Bunjes et al., 1995). As the differences in supramolecular structures of the polymorphs are likely to influence their drug incorporation capacity a proper characterization of lipid nanoparticles thus also entails a study of their polymorphic behavior.

The crystalline order of nanoparticles from simple triglycerides may prevent incorporation of appropriate amounts of drug molecules. The use of triglyceride mixtures has been considered to obtain particles with a less ordered matrix. Moreover, addition of a second matrix component may be useful to specifically alter the crystallization behavior of the lipid but may also affect other properties such as the particle size or structure of the matrix. For this reason, binary mixtures of trilaurin or trimyristin with tristearin are also studied. Knowledge about the behavior of such triglyceride mixtures may help to understand the processes in more complex triglyceride matrices.

2. Materials and methods

2.1. Materials

Dynasan 112 (trilaurin), 114 (trimyristin), 116 (tripalmitin), 118 (tristearin) were provided by Hüls AG (D-Witten). The purity of the fatty acid fraction is approximately 95% for Dynasan 114 and 116 and 99% for Dynasan 112 and 118. The hydroxyl value is below 5 in all cases. The following materials were obtained from the indicated sources and used without further purification: Soya lecithin Lipoid S100 (Lipoid KG, D-Ludwigshafen), sodium glycocholate, menadione (Sigma), tyloxapol USP (Sterling Organics), thiomersal (Synopharm), glycerol 85% Ph. Eur. III, bidistilled water.

Table 1
Preparation parameters and particle size of triglyceride dispersions

System	Composition of lipid matrix	Emulsifier composition	Temperature of preparation (°C)	Approximated PCS mean particle size by number (nm)
12a	D112	a	70	108
12b	D112	b	70	61
14a	D114	a	75	109[a], 116[b]
14b	D114	b	80	73[a], 93[b]
14bdl	98% D114, 2% menadione	b	70	72[a], 91[b]
16a	D116	a	80	144
16b	D116	b	80	87
18a	D118	a	90	136
18b	D118	b	80	139
1218M1	25% D112, 75% D118	a	80	134
1218M2	50% D112, 50% D118	a	80	116
1218M3	75% D112, 25% D118	a	80	112
1418M1	10% D114, 90% D118	b	80	101
1418M2	20% D114, 80% D118	b	80	106
1418M3	30% D114, 70% D118	b	80	93
1418M4	40% D114, 60% D118	b	80	100
1418M5a	50% D114, 50% D118	a	80	141
1418M5b	50% D114, 50% D118	b	80	118
1418M6	60% D114, 40% D118	b	80	103
1418M7	70% D114, 30% D118	b	80	120
1418M8	80% D114, 20% D118	b	80	113
1418M9	90% D114, 10% D118	b	80	112

D112, D114, D116, D114: Dynasan 112 (trilaurin), 114 (trimyristin), 116 (tripalmitin), 118 (tristearin). Emulsifier composition: (a) 1.6% phospholipid Lipoid S100, 0.4% sodium glycocholate; (b) 2% phospholipid Lipoid S100, 2% tyloxapol.
[a]Stored at room temperature.
[b]Stored at refrigerator temperature.

2.2. Sample preparation

The lipids were heated to at least 10°C above their melting point. The phospholipid was dispersed in the melt by probe sonication (MSE Soniprep 150) until the dispersion appeared clear. For the drug incorporation study, 2% menadione (related to the triglyceride phase) was dissolved in the triglyceride-phospholipid mixture. The co-emulsifier was dissolved in the aqueous phase containing 0.01% thiomersal as a preservative and 2.25% glycerol for isotonization. A predispersion of the lipid in this aqueous phase previously heated to approximately the same temperature as the lipid melt was prepared by probe sonication. This crude emulsion was passed through a thermostatized high-pressure homogenizer (Micron Lab 40) for 5 cycles at 800 bar. The hot dispersions were filtered through 0.45-μm filters and allowed to cool down to room temperature. Dispersions of monoacid triglycerides were split into two fractions one of which was stored at room temperature (20–25°C), the other was cold stored at 4–8°C. Of the binary mixtures only cold stored samples were under investigation. The exact compositions and preparation parameters are given in Table 1.

2.3. Particle size determination

Particle sizes were analyzed by photon correlation spectroscopy (PCS) with a Zetasizer 3 (Malvern Instruments) calculating the size distribution assuming spherical particles applying exponential sampling without Mie correction. The mean particle size was calculated from the num-

ber distribution as the diameter of the equivalent hydrodynamic sphere. The values given in Table 1 are the mean of five measurements.

2.4. Differential scanning calorimetry (DSC)

Thermal analysis was performed in a Perkin Elmer DSC 2-C calorimeter equipped with a Thermal Analysis Data Station 3700 using accurately weighed samples of 1–2 mg for bulk material or 10–20 mg for dispersions. Heating curves were recorded with a scan rate of 5 or 10°C/min. For the recrystallization studies, the samples were kept around 20°C above their melting point for at least 10 min and then cooled at 5°C/min.

The melting and recrystallization temperatures given correspond to the maxima or minima, respectively, in the DSC curves. Supercooling is given as the difference between these two temperatures. Since the curves are difficult to analyze quantitatively the values given below are approximate ($\pm$ 1 J/g). Polymorphic forms were assigned by correlation with the X-ray data.

2.5. Synchrotron radiation X-ray diffraction

Measurements were performed on the double focusing monochromator mirror camera X33 (Koch and Bordas, 1983) of the EMBL in HASYLAB on the storage ring DORIS III of the Deutsches Elektronen Synchrotron (DESY) at Hamburg. Two linear delay line readout detectors were connected in series to simultaneously monitor the small and wide angle diffraction patterns (Rapp et al., 1995) using standard data acquisition and evaluation systems (Boulin et al., 1986; Boulin et al., 1988). Data reduction and background subtraction was done following standard procedures (Koch, 1991) using the program SAPOKO (Svergun and Koch, unpublished). The scattering of water was subtracted from the diffraction pattern of the dispersions.

The scattering pattern of the particles was recorded at 20°C in three separate 1 min time frames to check for beam stability and radiation damage. The sample cells were thermostatized with a Huber waterbath controlled by an IF232 programmable interface. For the recrystallization studies the nanoparticles were held at about 20°C above their melting point for at least 10 min and then rapidly cooled to at least 5°C above the onset of crystallization. They were then further cooled at constant rates between 0.3 and 0.4°C/min and the scattering pattern was monitored continuously in 1 min time frames. The melting behavior was investigated by either heating the samples in 3°C steps and monitoring the scattering pattern for each single temperature step or by heating the samples at a constant rate of 1°C/min and recording the scattering pattern every minute.

2.6. Polarized light microscopy

The drug-loaded dispersions were examined in a Zeiss microscope III (Zeiss, D-Oberkochem) equipped with crossed polarizers and a λ-sheet.

3. Results

3.1. Characterization of raw materials

The thermoanalytical parameters of the bulk materials as derived from DSC measurements are given in Table 2. The X-ray diffraction patterns of all four materials display wide angle reflections at 0.53, 0.46, 0.39 and 0.37 nm typical of the β-form of triglycerides. The spacings of the small angle reflections (Table 3) are also in good agreement with the data given in the literature for the β-form (Chapman, 1962). Additional weak reflections at 3.77 nm in the trilaurin pattern and at 4.28 nm in the trimyristin pattern due to slight contaminations of unknown origin were also observed.

Small angle patterns of powder mixtures of tristearin with trimyristin or trilaurin, respectively, display the reflections of the corresponding raw materials. The reflection intensities approximately correlate with the mixing ratios.

3.2. Particle size of dispersions

Samples of all compositions yield approximated mean particle sizes between 60 and 150 nm (Table 1). For saturated monoacid triglycerides, the size

Table 2
Melting and crystallization parameters of triglyceride materials in bulk and in dispersions

System	Melting temperature (°C)			ΔH fus. β (J/g)	Crystallization temperature (°C)	ΔH recryst. α (J/g)
	α-form		β-form			
	Literature[a]					
D112		15	46	178	11	98
D114		33	56	181	28	105
D116	46	44.7	64	188	42	120
D118	55	54	73	200	51	124
12a			43	15	−9	10
12b			43	15	−8	12
14a			53	17	9	12
14b			53	18	8	15
16a	44		59[b]	19[c]	21	14
16b			60	20	21	15
18a	54		68	20[c]	30	15
18b	54		68	21[c]	30	14

[a]Chapman, 1962.
[b]Asymmetric maximum.
[c]May contain residual α-form.

tends to increase with triglyceride chain length. The size of cold stored trimyristin particles is larger than that of those stored at room temperature.

Stabilization with a phospholipid/tyloxapol blend usually yields smaller particles than with a phospholipid/bile salt blend, except in the tristearin system where the two emulsifier blends give similar particle sizes.

The sizes of particles obtained from binary mixtures are in the same range as those from pure triglycerides but without a clear dependence on mixing ratio. The particle sizes in the menadione-containing dispersion are comparable to those of the corresponding drug-free dispersion.

3.3. Monoacid triglyceride dispersions

3.3.1. DSC

The thermal curves of the tristearin and tripalmitin nanoparticles stored at room and refrigerator temperature display pronounced melting peaks. For trimyristin particles melting events are only detected in cold stored samples but not in samples stored at room temperature, even after several months of storage.

Trilaurin particles usually do not display an endothermal event even when cold stored for more than 5 months. Small fluctuations near the melting point of trilaurin in some DSC heating curves of these dispersions cold stored for several months cannot be unambiguously assigned to a melting event. In contrast to particles from the other triglycerides, dispersed trilaurin can only be crystallized at subzero temperatures (Table 2; Fig. 1).

The lipid nanocrystals from all four compounds melt about 3–5°C lower than the corresponding bulk material and the melting endotherms are broader. Melting curves of nanoparticles often display several side maxima or shoulders, especially when recorded at 5°C/min. Crystallization takes place at temperatures about 20°C lower than in the bulk. The supercooling increases from about 38°C for tripalmitin and tristearin dispersions to about 51°C for the trilaurin dispersion. The crystallization enthalpy is in all cases lower than the melting enthalpy, suggesting that crystallization and melting may occur in different polymorphs.

The fraction of the metastable α-form determined from the melting curves recorded 3 h after

Table 3
X-ray long spacings of raw materials and simple triglyceride dispersions

System	Spacing(nm)			
	β-form		α-form	
	Measured	Literature[a]	Measured[b]	Literature[a]
D112	3.12	3.12		3.56
D114	3.58	3.58		4.12
D116	4.06	4.06		4.56
D118	4.48	4.50		5.06
12a	(3.16)[c]			
12b	—			
14a	3.64		4.04	
14b	3.65[d]			
16a	4.09		4.52	
16b	4.12			
18a	4.58		5.03	
18b	4.55			

With exception of the tripalmitin dispersions values were obtained from cold stored dispersions.
[a]Chapman, 1962.
[b]Upon recrystallization.
[c]Very weak reflection only observed in a single experiment.
[d]Very asymmetric reflection (mean value).

preparation of phospholipid/bile salt stabilized dispersions is lower for tripalmitin than for tristearin nanoparticles (Fig. 2). A shoulder in the main melting peak may be due to a β′-fraction. In contrast, trimyristin and trilaurin particles do not seem to contain residues of their α-polymorph even upon immediate reheating after crystallization.

3.3.2. X-ray diffraction

The scattering patterns of all tristearin and tripalmitin dispersions give reflections characteristic of crystalline material, whereas with trimyristin dispersions crystalline material is found only in cold stored samples. Trimyristin particles stabilized with the phospholipid/tyloxapol blend display a very asymmetric small angle reflection. Trilaurin dispersions usually do not display any X-ray reflections. Only in a single measurement of the cold stored phospholipid/bile salt stabilized sample a very weak small angle but no detectable wide angle reflection was observed indicating crystallization of a negligible fraction of trilaurin. In general, the X-ray reflections of the nanoparticle dispersions are broader and much weaker than those of the bulk material. The position of the reflections is comparable to that of the bulk material in the β-form (Table 3) but the small angle spacings of the dispersions tend to be slightly larger.

Crystallization studies were performed with the phospholipid/bile salt stabilized trimyristin, tripalmitin and tristearin nanoparticles. The trilaurin dispersion was not investigated since the low crystallization temperature of dispersed trilaurin leads to experimental difficulties such as the risk of crystallization of the continuous phase. Moreover, crystallization of trilaurin particles is unlikely to occur under common production conditions. Upon crystallization of triglyceride nanoparticles, the wide angle reflections of the α-polymorph appear first. The corresponding small angle spacings are similar to those of the α-form given in the literature. The transition into the β-polymorph is completed within a few minutes in the trimyristin dispersion. The tristearin dispersion remains largely in the α-modification during the time course of the experiment (25 min

after recrystallization) and the tripalmitin dispersion has an intermediate behavior. The reflection patterns seem to consist of α- and β-reflections and combinations thereof without reflections which could be unambiguously assigned to the β'-modification (Fig. 3).

3.3.3. Drug loaded dispersion

Incorporation of menadione in a trimyristin dispersion leads to sedimentation of needle-like drug crystals in the aqueous phase if the dispersion is refrigerated thereby inducing crystallization of the trimyristin particles as confirmed by DSC. In contrast, the menadione-loaded dispersion stored at room temperature which does not give a DSC melting endotherm as typical for emulsions of supercooled melts appears homogenous and is isotropic under the polarizing microscope.

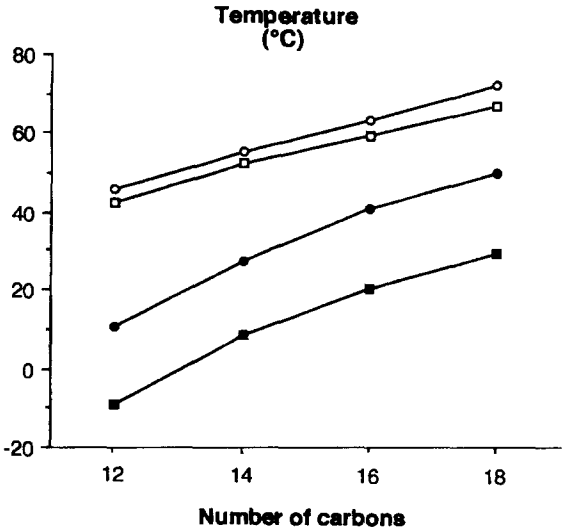

Fig. 1. Melting (open symbols) and crystallization (full symbols) temperatures of triglyceride bulk material (circles) and nanoparticles (squares) in dependence on the triglyceride chain lengths.

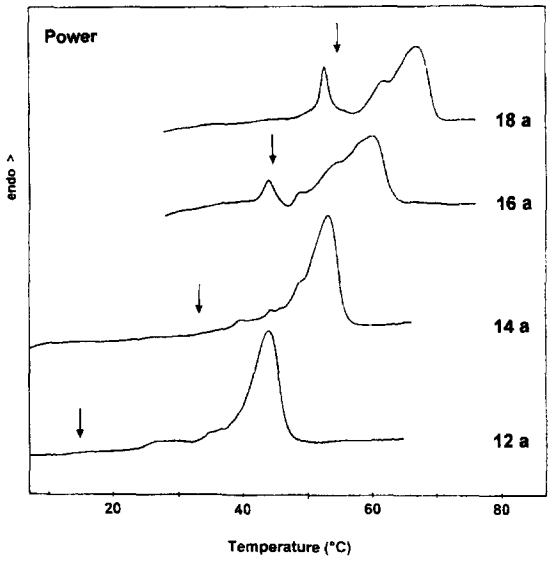

Fig. 2. DSC melting curves of nanoparticles prepared from tristearin (18a), tripalmitin (16a), trimyristin (14a) and trilaurin (12a). The curves were recorded 3 h after preparation (18a, 16a) or directly after crystallization of the particles (14a, 12a). The arrows indicate the α-melting temperatures of bulk material after (Chapman, 1962). The curves have been displaced along the ordinate for better visualization.

3.4. Nanoparticles from binary mixtures of monoacid triglycerides

3.4.1. Trimyristin/tristearin mixtures

3.4.1.1. DSC. In the heating curves there is a melting event between 37 and 74°C. In samples containing 30 to 80% tristearin two main melting maxima around 54 and 66°C (Fig. 4) as well as several other small maxima and shoulders can be observed. The melting enthalpies lie between those of simple trimyristin and tristearin dispersions without obvious dependence on mixing ratio (Fig. 5). The relative intensity of the maximum at higher temperatures increases with tristearin concentration. The melting enthalpy and the temperatures of melting maxima of a dispersed mixture containing 50% tristearin stabilized with phospholipid/bile salt are in the same range of order as for the analogous phospholipid/tyloxapol stabilized sample. The relative intensity of the melting maximum at higher temperatures is, however, more pronounced in the phospholipid/bile salt stabilized sample.

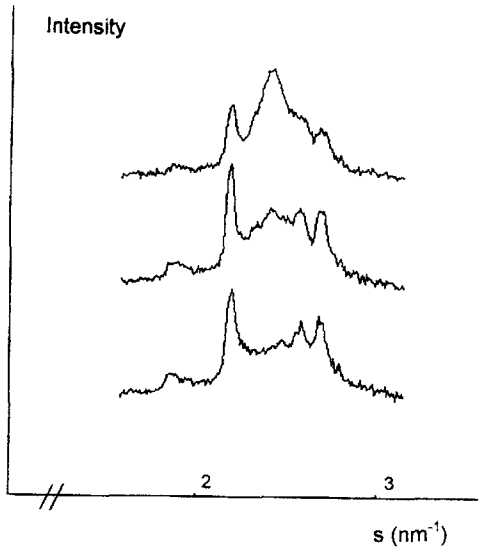

Fig. 3. Wide angle X-ray diffractograms of tristearin (top), tripalmitin (middle) and trimyristin (bottom) nanoparticle dispersions 18 min after crystallization from the melt. The patterns have been displaced along the ordinate for better visualization.

Recrystallization from the melt occurs in a single, sharp event. The recrystallization temperature increases almost linearly with increasing tristearin concentration although the effect seems to saturate at higher tristearin contents (Fig. 6).

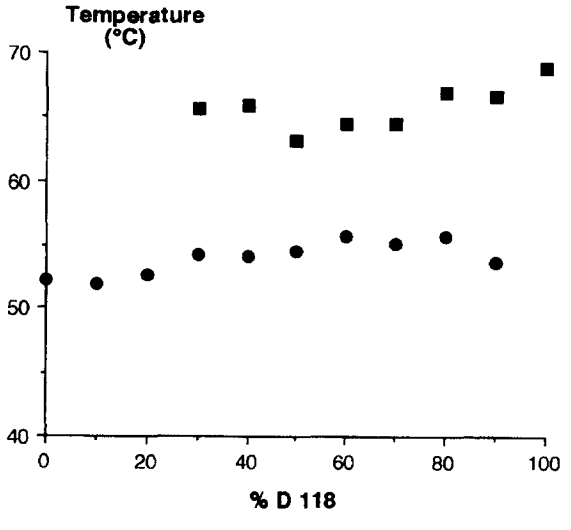

Fig. 4. Melting diagram of nanoparticle dispersions prepared from binary trimyristin/tristearin mixtures vs. tristearin (D118) content.

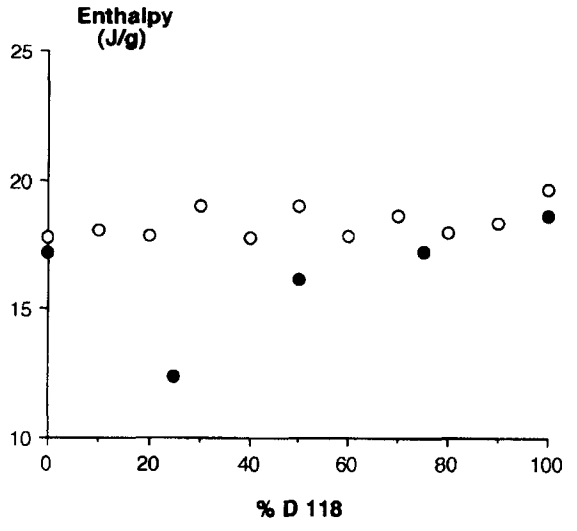

Fig. 5. Melting enthalpy of nanoparticle dispersions prepared from binary triglyceride mixtures (trilaurin/tristearin: full circles; trimyristin/tristearin: open circles) vs. tristearin (D118) content.

3.4.1.2. X-ray diffraction. All patterns display the wide angle reflections of the β-form and a single

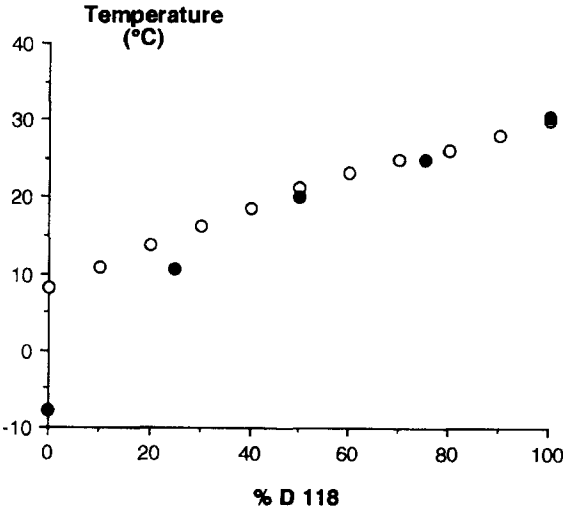

Fig. 6. Crystallization temperature of nanoparticles prepared from binary triglyceride mixtures (trilaurin/tristearin: full circles; trimyristin/tristearin: open circles) vs. tristearin (D118) content.

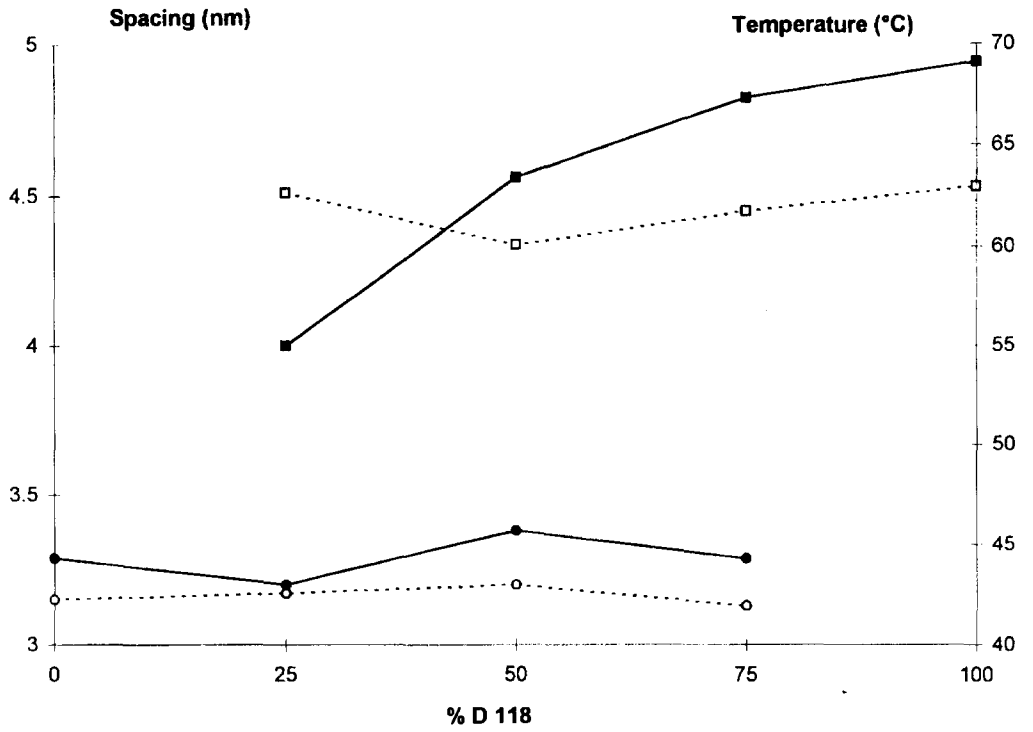

Fig. 7. Melting temperatures (full symbols) and long spacings (open symbols) of nanoparticle dispersions prepared from binary trilaurin/tristearin mixtures vs. tristearin (D118) content.

small angle reflection. The d-value of this reflection increases almost linearly with tristearin concentration, whereas the asymmetry of the peak increases with trimyristin concentration. The area of the small angle reflection is nearly constant in all samples but the reflections tend to be broader than those of simple trimyristin and tristearin dispersions. The pattern of the dispersion stabilized with the phospholipid/bile salt blend is similar to those of the phospholipid/tyloxapol stabilized series but has a symmetric small angle reflection.

Heating scans were performed on samples containing 50% tristearin. The intensity of the small angle reflection of the dispersion stabilized with the phospholipid/bile salt blend decreases above 40°C. From 49°C onwards it shifts from about 4.2 to about 4.5 nm at 61°C and finally disappears above 64°C. With the phospholipid/tyloxapol stabilized sample the intensity of the small angle reflection decreases above 46°C. Between 49 and 58°C the peak shifts from about 4.1 to 4.25 nm and disappears above 64°C.

During recrystallization of the phospholipid/bile salt stabilized 50% tristearin particles a single small angle reflection related to the α-modification appears at about 24°C and the wide angle reflection pattern subsequently changes to that of an α/β- mixture.

3.4.2. Mixtures of trilaurin and tristearin

3.4.2.1. DSC. Melting starts around 32°C and there are two endotherms in the melting curve. The first endotherm is similar to that of a crystallized trilaurin dispersion, whereas the temperature of the second increases with tristearin concentration (Fig. 7). The relative intensity of the melting peak near 45°C increases with trilaurin concentration and that of the second maximum with tristearin concentration.

The melting enthalpy tends to increase with tristearin concentration and is especially low in the sample containing 25% tristearin (Fig. 5). The sample with 75% tristearin approaches a melting enthalpy close to that of a simple tristearin dispersion.

The temperature of the main recrystallization event increases non-linearly with tristearin concentration (Fig. 6). The increase proceeds more rapidly at lower tristearin concentrations. Recrystallization does not occur as a single event in all cases but the exotherms of the samples containing 25 and 50% tristearin display a small side minimum around −1 and 6.5°C, respectively.

If the samples are reheated immediately after recrystallization an additional melting maximum at about 26°C is observed in the samples containing 25 and 50% tristearin. This additional peak which is more pronounced in the 25% tristearin mixture is not observed in aged samples.

3.4.2.2. X-ray diffraction. All samples give wide angle reflections typical of the β-form, whereas at small angles there is a double peak resulting from two crystal populations with different long spacings (Fig. 7). The d-values of the two compounds lie in the region of those of tristearin and trilaurin but without obvious dependence on mixing ratio. They can be assigned to a tristearin- and a trilaurin-rich form. The intensities of the two maxima depend on the tristearin/trilaurin mixing ratio of the particles but not exactly in proportion: in the mixture containing 50% tristearin the intensity of the maximum is higher for the tristearin-rich than for the trilaurin-rich form. In the sample containing 75% tristearin the longer spacing compound dominates the spectrum and there is only a very small shoulder at larger angles corresponding to the trilaurin-rich form. In contrast, the tristearin-rich form gives a distinct, broad reflection beside a larger peak in the sample containing 25% tristearin.

The intensity of the wide angle reflection at 0.46 nm is in the same range for the samples containing 50 and 75% tristearin and comparable to that of a pure tristearin dispersion, whereas that of the sample containing 25% tristearin tends to be lower.

When the samples are heated the reflection around 3.15 nm disappears first. After melting of the trilaurin-rich compound the reflection near 4.5 nm seems to be shifted to slightly smaller angles.

When particles containing 25 and 50% tristearin crystallize from the melt the two small angle reflections appear simultaneously. In the dispersion containing 75% tristearin the peak around 3.15 nm is barely resolved upon crystallization. In the corresponding wide angle patterns reflections at 0.46 and 0.415 nm characteristic of the β and α-form, respectively, also appear simultaneously. Upon further cooling the reflection intensities increase and additional β-reflections at 0.37 and 0.39 nm appear. The course of the subsequent polymorphic transitions is different in the various mixtures.

The small angle spacings of the 25% tristearin sample do not change. The intensity of the wide angle β-reflections slightly increases without distinct decrease in α-fraction with time. At the end of the experiment only the small angle spacing of the tristearin-rich compound is larger than in the β-form indicating that the α-fraction is due to the tristearin-rich compound.

In the mixture containing 50% tristearin, a slow transformation from the α- to the β-form is found in the wide angle reflection pattern and simultaneously the small angle spacings slightly decrease. About 30 min after crystallization residues of the α-form are still detectable in the wide angle pattern which can be attributed to the tristearin-rich form from the positions of the small angle spacings.

The spacing of the main small angle reflection in the 75% tristearin sample slightly decreases and the reflection becomes symmetric. The α-reflection at 0.415 nm disappears within 15 min and the peak positions in the crystallized sample are practically those of the β-form.

4. Discussion

4.1. Particle size

The trend to an increase in particle size with triglyceride chain length may be due to the in-

creasing viscosity of the triglyceride melts (Small, 1986). The differences in polarity of the molecules or the presence of partial glycerides should have a minor influence on the particle size as the interfacial phenomena are supposed to be dominated by the properties of the emulsifier.

The increase in trimyristin particle size of the cold stored dispersions compared to those stored at room temperature seems to be too small to be caused by agglomeration. It may rather be due to the shape of the crystalline cold stored particles. Nanocrystals of monoacid triglycerides such as tripalmitin are anisometric (Siekmann and Westesen, 1992) and thus have a larger frictional coefficient than spherical emulsion droplets of the same volume. This effect leads to an increase in hydrodynamic radius resulting in a larger mean PCS particle size. It is, therefore, difficult to compare particle sizes of liquid and crystalline particles directly.

The smaller particle sizes observed in phospholipid/tyloxapol-stabilized dispersions may partly be attributed to the higher surfactant/triglyceride ratio. Preparation of phospholipid/tyloxapol stabilized lipid nanoparticles requires larger amounts of emulsifier to obtain dispersions with homogenous size distributions than preparation with phospholipid/bile salt blends (Westesen et al., 1993; Siekmann and Westesen, 1994b). The comparatively large particle size of the phospholipid/tyloxapol stabilized tristearin particles may be due to the lower processing temperature of the tyloxapol stabilized system resulting in a higher viscosity of the tristearin melt.

Loading with menadione and drug expulsion from the carrier has no effect on the approximated mean PCS particle size.

4.2. Characteristics of dispersions

4.2.1. Monoacid triglycerides

Tristearin, tripalmitin and trimyristin are able to form nanoparticles with a crystalline lipid matrix after melt-homogenization but processing of trimyristin requires a cooling step after preparation. Trilaurin is not suitable for this kind of preparation since trilaurin dispersions remain emulsions even at refrigerator temperatures. The occurrence of a weak X-ray reflection or fluctuations in some melting curves of cold stored trilaurin dispersions might correspond to very small amounts of crystalline material. They may point to the onset of crystallization or be due to the presence of larger particles with higher crystallization tendency. Results on the properties of solid lipid nanoparticles prepared by melt-homogenization of trilaurin (Schwarz et al., 1994) should be interpreted with great care since they were probably obtained on dispersions of supercooled melts instead of solid particles. If dispersions of supercooled emulsion droplets are formed, they are thermodynamically metastable and crystallization may occur upon storage possibly leading to instabilities such as gel formation, particle growth or drug expulsion.

Although a glassy solid state of the supercooled triglyceride droplets cannot be completely excluded by the results of the present study such situation seems unlikely since the particles crystallize upon further cooling which is uncommon for glassy materials (Kerc and Srcic, 1995). While various techniques such as X-ray diffraction, DSC or electron microscopy can be used to distinguish between amorphous and crystalline material it is more difficult to discriminate between a liquid and a solid amorphous state. A glassy solid state can usually be detected by DSC but the low concentrations of dispersed material may limit the use of this method for colloidal dispersions. In contrast, nuclear magnetic resonance spectroscopy is a promising approach since it yields information on the mobility of the molecules (unpublished data). This method has also been applied successfully to the characterization of colloidal drug dispersions (Siekmann and Westesen, 1995).

The reduced melting temperature of colloidal lipid particles compared to the bulk has been attributed inter alia to their small size and the presence of surfactants (Siekmann and Westesen, 1994a). The melting point depression of nanoparticles observed in the present study is, however, smaller than that reported earlier for tripalmitin. It seems improbable that the large number of side maxima in some of the DSC melting curves is due to the coexistence of different polymorphs. Instead, they might result from the width of the size

distribution possibly resulting in particle fractions with different melting temperatures. This would also explain the large width of the melting peaks. The fact that melting of nanoparticles starts at lower temperatures than in the bulk has to be considered if particles are supposed to retain their solid state upon administration.

Supercooling occurs in all systems and is more pronounced in the dispersions than in the bulk. The higher degree of supercooling commonly observed in dispersions is attributed to the absence of nucleation centers in most of the particles above a critical crystallization temperature (Clausse, 1985). The high kinetic stability of the supercooled trilaurin and trimyristin droplets indicates that this effect may prevent crystallization for a considerable period of time.

The crystallization temperatures of the triglyceride nanoparticles are comparable to the lowest droplet freezing temperatures observed earlier for microscopic dispersions of these triglycerides (Phipps, 1964). Freezing at these temperatures was attributed to crystallization induced by homogenous nucleation. This explains why no significant influence of particle size on the crystallization temperature is observed here.

The difference between crystallization and melting temperature is larger for shorter-chain triglycerides, suggesting that nucleation may be enhanced in triglycerides with longer chains. It has to be considered, however, that triglyceride nanoparticles crystallize in the α-polymorph but that melting occurs from the β-form. The degree of supercooling with respect to the α-form can be estimated by comparison of the particle crystallization temperature with α-melting literature data. This leads to an almost constant value of supercooling with respect to the α-form of around 24°C for all four triglycerides. The trend towards decreasing α-supercooling with decreasing chain length as reported earlier (Phipps, 1964) is thus not observed here.

The results obtained with the four model triglycerides emphasize the significance of the formation of supercooled melts during the preparation of lipid nanoparticles by melt-emulsification. Especially with low melting point compounds crystallization of the resulting nanoparticles under common storage conditions cannot be taken for granted. Since the properties of materials are significantly altered in the colloidally dispersed state it is difficult to directly deduce characteristics of nanoparticles from those of the bulk. All triglycerides investigated here crystallize at a temperature about 20°C lower than in the bulk when colloidally dispersed. Whether this correlation is a general trend also for other lipid materials has to be further investigated.

DSC and X-ray studies reveal that the polymorphic transitions in the nanoparticles are faster for shorter-chain triglycerides. Such behavior is also known for bulk triglycerides (e.g., Chapman, 1962) but the rate of the transitions is much lower in the bulk (Siekmann and Westesen, 1994a). Differences in transformation kinetics have to be considered in connection with drug loading since the less dense crystal lattice of metastable polymorphs should favor drug incorporation. Instability problems upon long term storage due to drug expulsion from the crystal lattice during transition into a more stable polymorph are more likely to occur in more slowly transforming triglycerides like tristearin but can almost be excluded for the rapidly transforming trimyristin. To be utilized as a carrier system with an improved incorporation capacity the α-form of tristearin would, however, have to be further stabilized to ensure high drug loads for a reasonable period of time.

4.2.2. Drug-loaded dispersion

Trimyristin nanoparticles are a good model system to study the impact of the physical state on the ability of lipid nanoparticles to incorporate foreign substances. Crystallization of menadione-loaded trimyristin particles leads to expulsion of drug from the lipid matrix. The incorporation capacity of the nanocrystals for menadione is obviously significantly lower than that of the supercooled emulsion droplets. Although these results demonstrate that the physical state is an important factor determining drug incorporation capacity they cannot be generalized. In all likelihood specific interactions between drug molecules and the nanoparticle matrix are also important as illustrated by the incorporation of large concentrations of ubidecarenone into tripalmitin disper-

sions (Westesen et al., 1993; Siekmann and Westesen, 1994a).

4.2.3. Binary triglyceride mixtures

4.2.3.1. Trimyristin/tristearin mixtures. Addition of tristearin to trimyristin raises the crystallization temperature of the particles but does not lead to a significant decrease in crystalline order. The X-ray diffraction patterns with a single wider small angle reflection suggest that only one mixed crystalline form containing both triglycerides is formed. Alternatively, it may be possible that there are two different crystal populations with very similar spacings which are not resolved under the experimental conditions.

The two thermal maxima in most DSC melting curves indicate melting of two different crystalline forms. This result is in agreement with the observation of different melting events in the X-ray heating scans of the 50% tristearin samples. The shift of the small angle X-ray reflection may be due to the disappearance of an underlying reflection leaving only the reflection of a tristearin-richer phase or may point to an increase in lattice spacing during the melting process. The two crystalline forms which are indicated by the two melting events may, however, not be present in the original particles. A higher melting form could be formed upon heating by fractionation or recrystallization processes.

Usually, simple saturated monoacid triglycerides have a eutectic phase behavior resulting from a limited mutual solubility in the solid state (Rossell, 1967; Timms, 1984) but for trilaurin/trimyristin mixtures the formation of continuous solid solutions has also been described (Precht and Greiff, 1978). The melting behavior of the particles from the trimyristin/tristearin concentration series appears to be inconsistent with that of a eutectic mixture and may suggest an extended range of solid solution. It seems possible that the mutual solubility of triglycerides is higher in nanoparticles than in the bulk or that the rapidly proceeding crystallization in a highly supercooled nanodroplet prevents fractionation of the lipids.

The melting ranges are similar for both samples in DSC as well as in the X-ray studies, but the ratios of the peak heights in DSC and the extent of the peak shift in the X-ray patterns upon heating are different in spite of a comparable composition of the lipid phase. These results point to an influence of the emulsifier composition on the nanoparticle structure (e.g., resulting in different composition of the structures within the particles).

4.2.3.2. Trilaurin/tristearin mixtures. The effect of tristearin addition on the crystallization temperature of the triglyceride mixture is more pronounced at lower tristearin concentrations suggesting that tristearin dominates the crystallization process in these dispersions. Upon crystallization, a lower-melting trilaurin-rich and a higher-melting tristearin-rich crystalline compound are formed simultaneously as indicated by the X-ray experiments. Although nucleation is induced by the longer-chain glyceride crystallization occurs below the melting temperature also of the shorter chain compound leading to immediate crystallization of both compounds within the same particle. Separate formation of trilaurin- and tristearin-rich particles upon crystallization would be thermodynamically unfavorable and should also lead to a pronounced decrease in mean particle size. The X-ray peak ratios indicate that the solubility of trilaurin in tristearin in nanoparticles is below 25% but much larger than the solubility of tristearin in trilaurin. The crystal lattice dimensions are not markedly affected by incorporation of the second matrix triglyceride. The formation of a mixed crystalline matrix leads to melting characteristics of a mixture with a eutectic temperature close to the melting point of trilaurin and a eutectic composition close to the lower melting compound. The melting diagram is qualitatively similar to that of trilaurin/tristearin mixtures in the bulk (Rossell, 1967). The low melting onset of trilaurin/tristearin nanoparticles would lead to a partial loss of the solid character upon administration.

The comparatively low melting enthalpy and X-ray reflection intensities of the sample with only 25% tristearin may indicate that not all material has crystallized in this sample and that a critical amount of tristearin may be necessary to induce

complete crystallization. The side maximum in the DSC cooling curves of samples with lower tristearin content may point to a second crystallization process or a polymorphic transition.

The different time course of polymorphic transitions in samples with different mixing ratios can be correlated with the crystallization temperatures. The sample with high tristearin concentration transforms extremely rapidly into the stable β-form although the transformation of pure tristearin particles is very slow. Particles with 25 and 50% tristearin transform much more slowly and still contain residues of a tristearin-rich α-form at the end of the X-ray crystallization experiments which are also detected in DSC-curves of freshly crystallized samples. The pronounced melting point depression of this α-form compared to that of α-tristearin is probably due to the formation of a solid solution of trilaurin in tristearin. As the crystallization of the sample with 75% tristearin occurs at temperatures around this α-melting point only small amounts of the α-polymorph are formed which rapidly transform into the β-polymorph. The crystallization temperature of the other samples is below the α-melting point of the tristearin-rich phase and the α-form is, therefore, more stable. The transformation seems to be slowest in the 25% tristearin sample. The low temperatures after crystallization, especially of the 25% tristearin sample, may further slow down the transition kinetics of the tristearin-rich compound. The β-reflections which appear directly upon crystallization of the particles containing 25 and 50% tristearin are probably due to the trilaurin-rich component. These particles crystallize around the trilaurin α-melting temperature at which the trilaurin α-form is unstable and transforms rapidly into the stable β-polymorph.

5. Conclusions

The investigation of the four simple triglycerides demonstrates that the suitability of triglycerides for the formation of solid lipid nanoparticles cannot directly be deduced from their bulk properties. Even if the materials are in principle able to form solid nanoparticles their crystallization behavior in the dispersed state has to be studied carefully to optimize the temperature control of the production process. This temperature control should not only include the melt-homogenization process itself but also a cooling step that leads to the solidification of the nanoparticles.

The pronounced tendency of colloidally dispersed triglycerides towards the formation of supercooled melts with a considerable kinetic stability can be utilized to evaluate the differences between colloidal emulsions and suspensions. Especially trimyristin nanoparticles seem to be suitable for this purpose as they can be easily obtained and stored in the liquid as well as in the solid state.

The presence of triglycerides with longer hydrocarbon chains seems to catalyze the nucleation of triglycerides with low crystallization tendency. Addition of longer-chain triglycerides such as tristearin may thus help to overcome solidification problems in lower melting triglyceride nanoparticles. It should be kept in mind, however, that addition of a second matrix component alters the nanoparticle structure and further complicates the crystallization processes. In particular the course of polymorphic transitions may be different in mixed particles as demonstrated for trilaurin/tristearin mixtures.

A considerable intersolubility of simple monoacid triglycerides, which is, however, not accompanied by a drastic decrease in crystallinity, seems to be possible in mixed triglyceride nanoparticles. If the preparation of lipid nanoparticles with a less ordered crystal lattice is intended, the use of more complex fat mixtures should be considered. The particles of binary mixtures investigated in the present study can be regarded as simple model systems for complex lipid mixtures and may help to understand their behavior. If the binary particles are taken as a simplified model for the interaction of a second component with a triglyceride matrix the data indicate that incorporation of larger amounts of most foreign substances into the crystal lattice will be quite difficult to achieve since even structurally related substances tend to phase separate within the particles.

Acknowledgements

The authors thank Hüls AG, D-Witten, and Lipoid KG, D-Ludwigshafen, for supply of raw materials. H.B. and K.W. thank Pharmacia Oncology Immunology AB, S-Helsingborg, for financial support.

References

Boulin, C.J., Gabriel, A. and Koch, M.H.J., Data acquisition systems for linear and area X-ray detectors using delay line readout. *Nucl. Instrum. Methods Phys. Res.*, A269 (1988) 312–320.

Boulin, C., Kempf, R., Koch, M.H.J. and McLaughlin, S.M., Data appraisal, evaluation and display for synchrotron radiation experiments: hardware and software. *Nucl. Instrum. Methods*, A249 (1986) 399–407.

Bunjes, H., Westesen, K. and Koch M.H.J., Complex fats as matrix constituents in lipid nanoparticles. *Proc. 1st World Meeting APGI/APV*, (1995) 497–498.

Chapman, D., The polymorphism of glycerides. *Chem. Rev.*, 62 (1962), 433–456.

Clausse, D., Research techniques utilizing emulsions. In Becher, P. (Ed.), *Encyclopedia of Emulsion Technology*, Vol. III, Marcel Dekker, New York, 1985, pp. 77–157.

Kerc, J. and Srcic, S., Thermal analysis of glassy pharmaceuticals. *Thermochim. Acta*, 248 (1995) 81–95.

Koch, M.H.J., Scattering from non-crystalline systems. In Ebashi, S., Koch, M.H.J. and Rubenstein, E. (Eds.), *Handbook on Synchrotron Radiation*, Elsevier, Amsterdam, 1991, pp. 241–267.

Koch, M.H.J. and Bordas, J., X-ray diffraction and scattering on disordered systems using synchrotron radiation. *Nucl. Instrum. Methods*, 208 (1983) 241–267.

Müller, R.H., Mehnert, W., Lucks, J.-S., Schwarz, C., zur Mühlen, A., Weyers, H., Freitas, C. and Rühl, D., Solid lipid nanoparticles (SLN) — an alternative colloidal carrier system for controlled drug delivery. *Eur. J. Pharm. Biopharm.*, 41 (1995) 62–69.

Phipps, L.W., Heterogeneous and homogenous nucleation in supercooled triglycerides and *n*-paraffins. *Trans. Faraday Soc.*, 60 (1964), 1873–1883.

Precht, D. and Greiff, R., Zur Mischkristallisation der Triglyceride unter besonderer Berücksichtigung der β-Modifikation. *Kieler Milchwirtsch. Forschungsber.*, 30 (1978), 157–178.

Rapp, G., Gabriel, A., Dosière, M. and Koch, M.H.J., A dual detector single readout system for simultaneous small (SAXS) and wide angle X-ray (WAXS) scattering. *Nucl. Instrum. Methods A*, 357 (1995) 178–182.

Rossell, J.B., Phase diagrams of triglyceride systems. In Paoletti, R. and Kritchevsky, D. (Eds.), *Advances in Lipid Research*, Vol. V, Academic Press, New York, 1967, pp. 353–408.

Schwarz, C., Mehnert, W., Lucks, J.S. and Müller, R.H., Solid lipid nanoparticles (SLN) for controlled drug delivery. I. Production, characterization and sterilization. *J. Controlled Release*, 30 (1994) 83–96.

Siekmann, B. and Westesen, K., Submicron-sized parenteral carrier systems based on solid lipids. *Pharm. Pharmacol. Lett.*, 1 (1992), 123–126.

Siekmann, B. and Westesen, K., Thermoanalysis of the recrystallization process of melt-homogenized glyceride nanoparticles. *Colloids Surf. B*, 3 (1994a) 159–175.

Siekmann, B. and Westesen, K., Melt-homogenized solid lipid nanoparticles stabilized by the nonionic surfactant tyloxapol: I. Preparation and particle size distribution. *Pharm. Pharmacol. Lett.*, 3 (1994b) 194–197.

Siekmann, B. and Westesen, K., Preparation and physicochemical characterization of aqueous dispersions of coenzyme Q_{10} nanoparticles. *Pharm. Res.*, 12 (1995) 201–208.

Small, D.M., The physical chemistry of lipids. In Hanahan, D.J. (Ed.), *Handbook of Lipid Research*, Vol. IV, Plenum Press, New York, 1986, 367–372.

Timms, R.E., Phase behavior of fats and their mixtures. *Prog. Lip. Res.*, 23 (1984), 1–38.

Westesen, K. and Bunjes, H., Do nanoparticles prepared from lipids solid at room temperature always possess a solid lipid matrix? *Int. J. Pharm.*, 115 (1995) 129–131.

Westesen, K., Siekmann, B. and Koch, M.H.J., Investigations on the physical state of lipid nanoparticles by synchrotron radiation X-ray diffraction. *Int. J. Pharm.*, 93 (1993) 189–199.